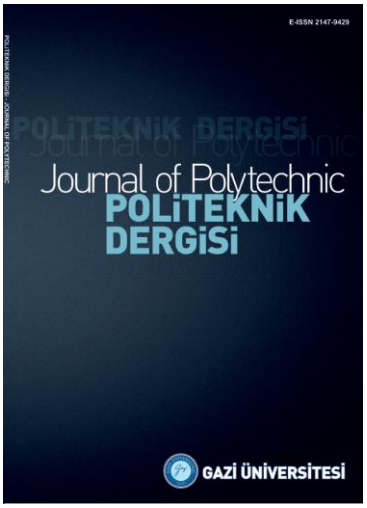

POLİTEKNİK DERGİSİ

JOURNAL of POLYTECHNIC

ISSN: 1302-0900 (PRINT), ISSN: 2147-9429 (ONLINE)
URL: http://dergipark.org.tr/politeknik

Development of a design methodology for a centrifugal compressor with the utilization of CFD

Radyal bir kompresör için HAD yardımıyla tasarım metodolojisi geliştirilmesi

***Yazarlar (Authors)**: Fatma Zeynep AYTAÇ[1], Nuri YÜCEL[2]*

ORCID[1]: 0000-0003-0717-5287

ORCID[2]: 0000-0001-9390-5877

Bu makaleye şu şekilde atıfta bulunabilirsiniz(To cite to this article): Aytaç F. Z. and Yücel N., "Development of a design methodology for a centrifugal compressor with the utilization of CFD", ***Politeknik Dergisi***, 23(1): 231-239, (2020).

Erişim linki (To link to this article): http://dergipark.org.tr/politeknik/archive

DOI: **10.2339/politeknik.658358**

Radyal Bir Kompresör için Hesaplamalı Akışkanlar Dinamiği Yardımıyla Tasarım Metodolojisi Geliştirilmesi

Araştırma Makalesi / Research Article

Fatma Zeynep AYTAÇ*, Nuri YÜCEL
Mühendislik Fakültesi, Makine Müh. Bölümü, Gazi Üniversitesi, Türkiye
(Geliş/Received : 11.03.2019 ; Kabul/Accepted : 24.06.2019)

ÖZ

Radyal kompresörler günümüzde çeşitli amaçlar için belirli sektörlerde yaygın olarak kullanılmaktadır. Havacılık ve savunma sektörlerinde ise çeşitli motor yapılarında akışkanın basıncını artırmak için kullanılmaktadır. Mevcut çalışmada, bir mini jet radyal kompresörü, Hesaplamalı Akışkanlar Dinamiği (HAD) araçları kullanılarak, geliştirilen metodoloji ile tasarlanmıştır. Tasarımı yapılan kompresörğn üretimi yapılmış ve yerli bir motor kullanılarak testi gerçekleştirilmiştir. Tasarım spesifikasyonları, test için kullanılan motor doğrultusunda belirlenmiş ve sonuçta belirlenen limitler içerisinde, 0.678 kg/s hava debisi, 6.6135 toplam basınç oranı ve %92.38 verim elde edilmiştir. Test sonucunda ise her ne kadar HAD sonuçları ve deney sonuçları arasında farklılık gözlemlendiyse de, elde edilen eğrilerin genel eğiliminin benzer olduğu gözlemlenmiş ve tasarım doğrulanmıştır.

Anahtar Kelimeler: Radyal kompresör, hesaplamalı akışkanlar dinamiği, tasarım metodolojisi, kompresör testi.

Development of a Design Methodology for a Centrifugal Compressor with the Utilization of CFD

ABSTRACT

Centrifugal compressors are widely used for several purposes in many industries. Aero defense industry uses these compressors in the engines of several structures. In the present study, the centrifugal compressor of a mini jet engine is designed with the utilization of Computational Fluid Dynamics (CFD) tools with the methodology developed. The designed compressor is manufactured and its tests were conducted using an engine that is being utilized commercially. The performance parameters of the designed compressor and the results obtained from the engine were compared and presented. The specifications of the designed compressor was determined in the light of the requirements of the test engine. It was observed that the obtained mass flow rate (0.678 kg/s), pressure ratio (4.6135) and the efficiency (92.38%) values are within the limits of the design specifications and the although there is a slight difference between the results of the CFD analyses and the experiments, the trends of the curves are consistent with each other.

Keywords: Centrifugal compressor, computational fluid dynamics, design methodology, compressor tests.

1. INTRODUCTION

Today, centrifugal compressors are widely used in many industries for several reasons such as aircraft industry for fluid compression, in gas turbines and in turbocharged combustion engines, etc [1]. Centrifugal compressors mainly increase the kinetic energy of the fluid within using a rotating impeller [2]. It is a mechanical device which is able to transfer the energy efficiently to the fluid medium so that it can be delivered in large quantities at several multiples of inlet pressure [3]. There are several advantages of centrifugal compressors to be preferred, such as their robustness, compactness, reliance, resistance to foreign object damage and wider operating range [3].

1.1. Basic Components

A centrifugal impeller has three main parts; the impeller, diffuser and the scroll. If the compressor has any inlet guide vanes, they are responsible from directing the fluid to the impeller in the right angle. Afterwards, the impeller increases the kinetic energy of the fluid in addition to the increment in the total and static pressures. Then, the fluid leaves the impeller and reaches to the diffuser, where its velocity is decreased and its static pressure is increased and the diffuser discharges the fluid to the scroll. The main idea of the design is to compress the fluid in the required amount while minimizing losses. The basic schematic of a centrifugal compressor is given in Figure 1.

*Sorumlu Yazar (Corresponding Author)
e-posta : zeynepaytac@gazi.edu.tr

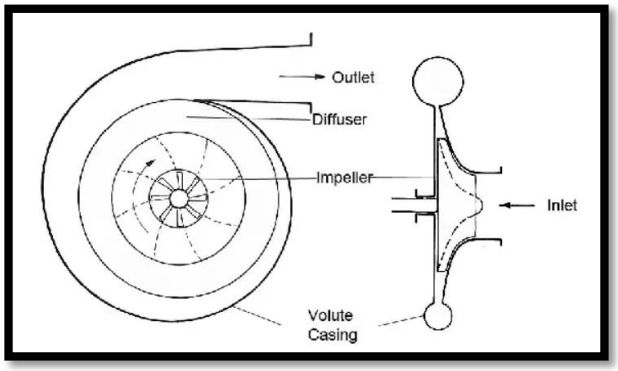

Figure 1. Schematic of a centrifugal compressor [4]

One can prefer two-dimensional or three-dimensional blade profiles while designing the impeller blades. While 2D-impellers are compatible for individual and small-scale production, 3D impellers provide the highest durability at high blade velocities and they are more effective at high Mach numbers and respectively big loading factors [5].

Respectively high pressure ratios in a centrifugal compressor end up in complicated flow characteristics which causes shock waves and finally they result in the deterioration of efficiency and operating range [6].

Compressor operating range is determined from the performance map which has the choke line and the surge line as the boundaries of the map. Performance map consists of efficiency lines determined in several rotating speeds between the surge and choke points at that speed. Here, surge is the phenomenon which occurs when the compressor is unable to produce the sufficient pressure to provide the continuous flow to the rest of the system. It is assumed that surge occurs below the minimum mass flow rate that the compressor can still operate with. Decreasing the mass flow further will result in surge which will lead to aerodynamic instabilities and finally in mechanical damage. Oppositely, choke point is the point where the compressor operates with the maximum mass flow rate of fluid; increasing the mass flow further will not serve the compressor's purpose and it will not be compressing the fluid any more. The designer should aim to maximize the distance between the choke and surge points while keeping the efficiency as high as possible.

In the present study, the design of a centrifugal compressor for a mini jet with the utilization of CFD tools is implemented and the designed compressor is manufactured. Using the manufactured compressor, the tests are conducted and later, the obtained results of the CFD analyses and the tests are compared with each other.

1.2. Utilization of CFD for Impeller Design

In the preliminary design process, one can only determine the inlet and outlet velocity triangles, blade angles and shapes. The intimate 3D profile of the blade is generated and analyzed by means of Computational Fluid Dynamics (CFD) tools. Today, as designing the impeller using experimental methods can be infeasible for many researchers, CFD tools are increasingly used in the design process of turbo machines; which provides the designer to save on effort, time and cost. CFD tools offers the designer a cost-effective and accurate way to get through the design process with respect to experimental methods [7]. However; due to the complex flow nature of these structures, the importance of the developed case becomes substantial in terms of accuracy.

1.3. Specifications of the Compressor

1.3.1. Dimensional Specifications

The dimensional specifications of the designed compressor is given in Table 1. The design procedure is conducted in the light of the specified information of several dimensions and tip profile. The fixed dimensions is given in Figure 2 and the specified tip profile is given in Figure 3.

Table 1. The dimensional specifications

Rotation Direction	The compressor is required to rotate clockwise from front view.
Dimensions	The fixed dimensions of the compressor are given in Figure 2.
Tip Profile	The tip profile of the compressor is fixed and is given in Figure 3.
Blade Number	The number of the blades is not allowed to be multiples of 6 or 8.
Weight	260 ± 15 g.
Material	Aluminum 2124 Alloy.

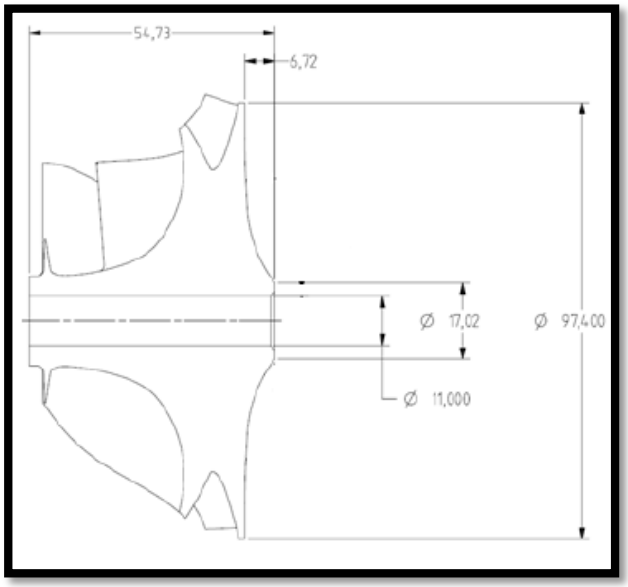

Figure 2. The specified dimensions of the compressor

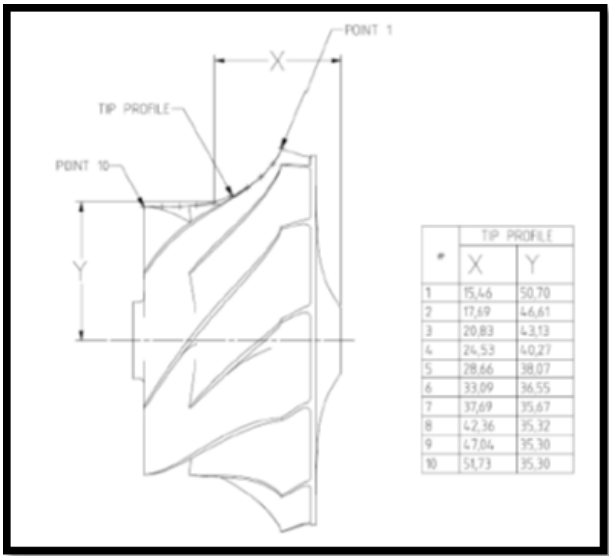

Figure 3. The required tip profile

1.3.2. Aerodynamic Specifications

The compressor is designed at sea level (101.325 kPa and 15°C) and the requirements are given in Table 2.

Table 2. The design inputs and requirements at design point

Design Inputs	Shaft Velocity	96000 rpm
	Inlet Total Pressure	101325 Pa
	Inlet Total Temperature	288.15 K
Design Requirements	Air Mass Flow Rate	0.68 ± 0.01 kg/s
	Total Pressure Ratio	4.6 ± 0.05
	Isentropic Efficiency	≥ 0.87
	Surge Margin	≥ 15

Surge margin is calculated according to Equation 1.

$$\left(\frac{PR_{stall}}{PR_{design}} \times \frac{\dot{m}_{design}}{\dot{m}_{stall}} - 1\right) \times 100 \quad (1)$$

2. MATERIAL AND METHOD

Each centrifugal compressor has its own design inputs and requirements depending on the purpose of utilization. Consequently, even though certain dimensions such as exducer diameter, blade height etc. can be the same, each compressor has a unique design. In order to simplify the design process, a design methodology is developed in the light of the research about centrifugal compressor theory, 3D design programs and CFD and FEA tools. Using the methodology given in Figure 4, different compressors for various purposes can be designed parametrically in a simple and systematic way.

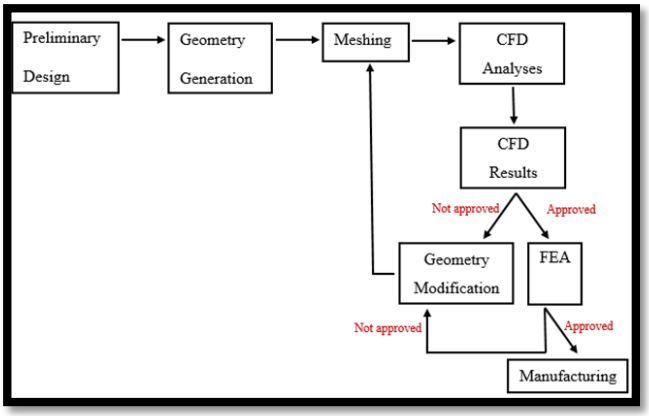

Figure 4. The outline of the design methodology

2.1. Preliminary Design

In order to generate the initial blade profile, it is necessary to determine the velocity triangles at the inlet hub, inlet shroud and outlet sections. To determine the velocity triangles, certain thermodynamic parameters such as total and static temperatures, total and static pressures, total and static densities and Mach numbers are calculated at the inlet and outlet. The calculated values are given in Table 3. It is assumed that the isentropic efficiency of the rotor is 87% and the air enters the impeller in a pure axial direction (no pre-whirl).

Table 3. The calculated thermodynamic parameters

Parameter	**Value**	**Unit**
P_1	84064.034	Pa
P_2	263349.065	Pa
P_{02}	466095	Pa
T_1	273.243	K
T_2	398.743	K
T_{02}	469.39	K
ρ_1	1.072	kg/m^3
ρ_2	2.307	kg/m^3
ρ_{02}	3.459	kg/m^3

The velocity triangles at the inlet hub, inlet shroud, inlet mean line and outlet sections are given in Figure 5. By taking into consideration the theoretical calculations and specifications, it was decided that the rotor has 7 main blades and 7 splitter blades.

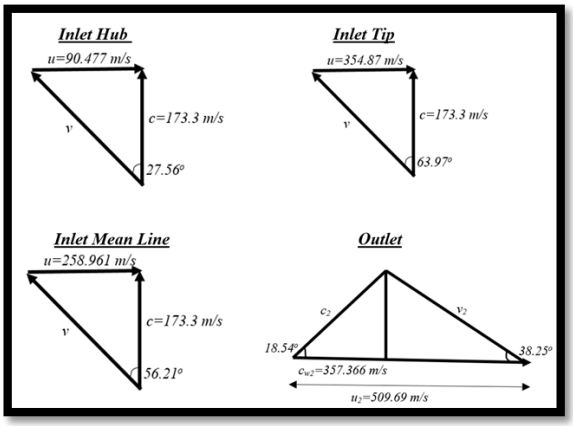

Figure 5. The velocity triangles

2.2. Geometry and Grid Generation

After the determination of the velocity triangles and blade angles, the next step is to generate the geometry. In this study, ANSYS Workbench 15.0 is used throughout the design process. The BladeGen module of the mentioned tool was utilized in order to generate the initial 2D blade geometry. The blade geometry (height, inducer diameter, exducer diameter, inlet and outlet blade angles, etc.) was formed in the light of the theoretical calculations, whereas the required tip profile and tip clearance value was dictated to the tool. In addition, blade thickness was determined so as to ensure the required aerodynamic and structural specifications. The 2D profile of the blade is given in Figure 6.

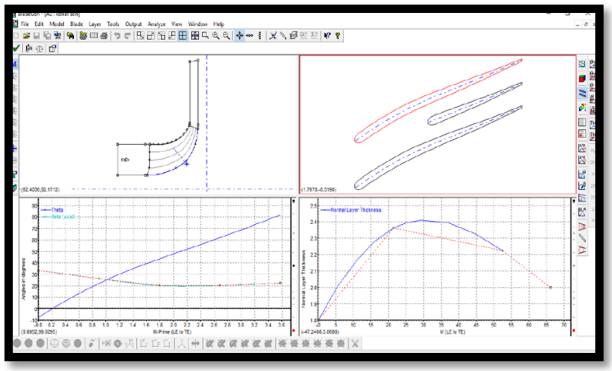

Figure 6. The ANSYS BladeGen view of the 2D blade profile

Here, the top left view represents the meridional profile of the blade. The left base view is the blade angle distribution window. With the help of this section, one can delicately change the blade angles at any sections. The base right window represents the blade thickness distribution; whereas the top right view is the blade-to-blade view of the compressor.

After the completion of the design process in BladeGen tool, the blade was divided into finite elements by using ANSYS TurboGrid. Here, by providing the enough number and quality of the solution grids, the accuracy of the solution is ensured. To determine the sufficient number After the completion of the design process in BladeGen tool, the blade was divided into finite elements by using ANSYS TurboGrid. Here, by providing the enough number and quality of the solution grids, the accuracy of the solution is ensured. To determine the sufficient number of grid cells, a mesh independence study was conducted and it was found out that approximately 900000 cells are enough to obtain an accurate solution. The mesh data is given in Table 4.

Table 4. Mesh Data

Number of Nodes (Total)	Number of Elements (Total)
1052236	991070

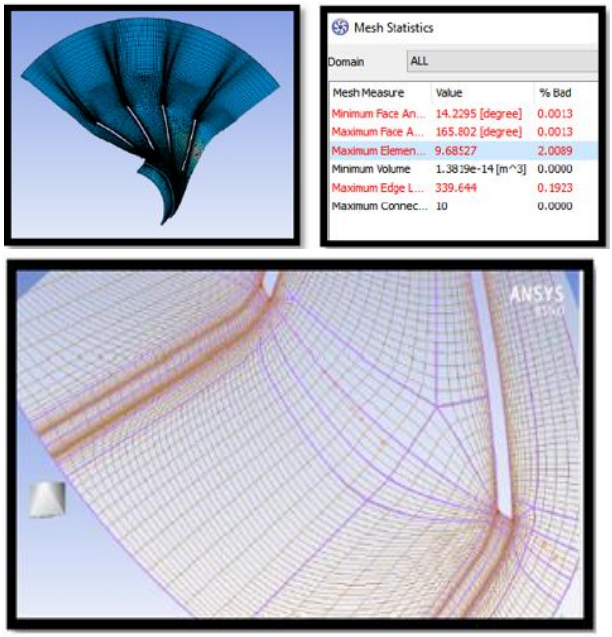

Figure 7. Blade grid structure

When generating the grid structure, special effort is made so that the mesh is enough dense near the boundary layer and becoming less dense gradually when getting away from that region. As can be seen from the mesh statistics in Figure 7, the error is negligible throughout the whole volume and the grids in the critical regions are denser with respect to other domains.

After the completion of the meshing process, ANSYS CFX 15 is used to set up the analysis.

2.3. Solver Settings and CFD Analyses

Navier – Stokes equations are sufficient to model the 3D motion of the fluid particle without any extra information needed.

2.3.1. Conservation of Mass

Consider a fluid particle having dimensions of dx, dy and dz. The mass conservation for such a particle is expressed with Equation 2. It states that the variation of net mass flow within a flow element is equal to the net mass flux passing through the boundaries of the element.

$$\frac{\partial \rho}{\partial t} + \frac{\partial (\rho u_i)}{\partial x_i} = 0 \quad (2)$$

2.3.2. Conservation of Momentum

Momentum conservation states that the amount of momentum variation on the unit mass of a fluid particle is equal to the sum of pressure variations, viscous forces and external forces. It is given in Equation 3.

$$\frac{D(u_i)}{Dt} = \frac{\partial u_i}{\partial t} + u_j \frac{\partial u_i}{\partial x_j} = -\frac{1}{\rho}\frac{\partial P}{\partial x_i} + \nu \frac{\partial^2 u_i}{\partial x_j^2} + F_i \quad (3)$$

The flow within the centrifugal compressor is simulated using Reynolds Averaged Navier – Stokes (RANS) equations. RANS methods are widely used in industrial applications [8]. In Reynolds averaging, the actual solution variables in Navier – Stokes equations are averaged depending on time after being decomposed into average and fluctuating components. The final equations are given in Equation 4.1, 4.2 and 4.3 in terms of x, y and z axes.

x-component:

$$\rho \frac{D\bar{u}}{Dt} = \rho[\frac{\partial}{\partial x}(\bar{u}^2) + \frac{\partial}{\partial y}(\bar{u}\bar{v}) + \frac{\partial}{\partial z}(\bar{u}\bar{w}) = \rho g_x - \frac{\partial \bar{P}}{\partial x} + \frac{\partial}{\partial x}\left[\mu \frac{\partial \bar{u}}{\partial x} - \rho\overline{u'^2}\right] + \frac{\partial}{\partial y}\left[\mu \frac{\partial \bar{u}}{\partial y} - \rho\overline{u'v'}\right] + \frac{\partial}{\partial z}\left[\mu \frac{\partial \bar{u}}{\partial z} - \rho\overline{u'w'}\right] \quad (4.1)$$

y-component:

$$\rho \frac{D\bar{v}}{Dt} = \rho[\frac{\partial}{\partial x}(\bar{u}\bar{v}) + \frac{\partial}{\partial y}(\bar{v}^2) + \frac{\partial}{\partial z}(\bar{v}\bar{w}) = \rho g_y - \frac{\partial \bar{P}}{\partial y} + \frac{\partial}{\partial x}\left[\mu \frac{\partial \bar{v}}{\partial x} - \rho\overline{u'v'}\right] + \frac{\partial}{\partial y}\left[\mu \frac{\partial \bar{v}}{\partial y} - \rho\overline{v'^2}\right] + \frac{\partial}{\partial z}\left[\mu \frac{\partial \bar{v}}{\partial z} - \rho\overline{v'w'}\right] \quad (4.2)$$

z-component:

$$\rho \frac{D\bar{w}}{Dt} = \rho[\frac{\partial}{\partial x}(\bar{u}\bar{w}) + \frac{\partial}{\partial y}(\bar{v}\bar{w}) + \frac{\partial}{\partial z}(\bar{w}^2) = \rho g_z - \frac{\partial \bar{P}}{\partial z} + \frac{\partial}{\partial x}\left[\mu \frac{\partial \bar{w}}{\partial x} - \rho\overline{u'w'}\right] + \frac{\partial}{\partial y}\left[\mu \frac{\partial w}{\partial y} - \rho\overline{v'w'}\right] + \frac{\partial}{\partial z}\left[\mu \frac{\partial \bar{w}}{\partial z} - \rho\overline{w'^2}\right] \quad (4.3)$$

2.3.3. Turbulence Model

Turbulence consists of fluctuations in time and space in flow area. It is a 3D, time-dependent and highly complex structure which can cause in distinct variations in flow characteristics. It appears when the inertial forces overcome viscous forces on a fluid. Although it is simplified by the conservation equations and the averaging procedure, these equations are not sufficient to resolve the flow accurately. As a result, the two equations coming from turbulence models are required to solve the flow accurately in addition to RANS equations. On the present study, k-ω SST model is used with the RANS equations. It is widely preferred in turbo machinery simulations involving rotating structures. Although standard k – ω model over predicts separation, k – ω SST does not face with this problem.

2.3.4. Simulation

NSYS CFX-Pre is used to set up the analyses and ANSYS CFX Solver is used to run the cases. The regions used to define the boundary conditions are given in Figure 8.

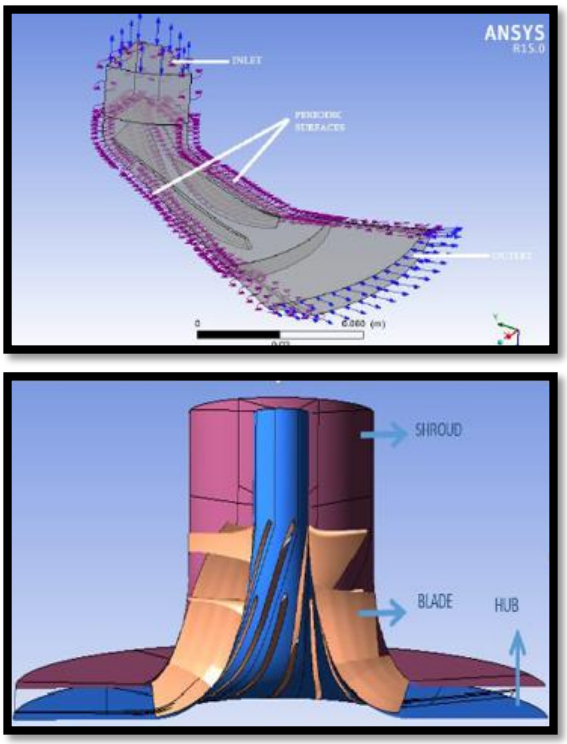

Figure 8. The regions used for setting up the boundary conditions for the CFD analyses

To reduce the computation time and effort, only one passage consisting of one main blade and one splitter is used and as can be seen from Figure 8, periodic surfaces are defined at each side of the passage. The inlet and outlet boundary types are selected as "Opening". As the rotation speed of the compressor is notably high, CFX compels these regions to be inlet and outlet when these types are selected. When "inlet" and "outlet" type boundaries are selected, backflow occurs, which deteriorates the performance and so, the required flow and performance goals cannot be achieved. By choosing this boundary types as "Opening", the obligations on the flow disappear and more realistic results are obtained.

As given, a pressure of 101.325 kPa and a temperature of 288.15 K is given at the inlet and a pressure of 360 kPa and 470 K is given at the outlet. The values given at the outlet region is determined from the theoretical calculations. The reference pressure is chosen as 0 atm. The fluid is air – ideal gas and the rotational speed is

96000 rpm. As known from literature that k-ω SST turbulence model is more accurate for rotating structures, this model is used for the analyses, as mentioned before. The residual target is specified as 10-8. Furthermore, several monitor points was used to monitor the mass flow rate value at the outlet and to monitor the total pressure rate in order to check the convergence.

After setting up the cases, analyses were conducted using CFX Solver Manager and the results are evaluated. The analyses are repeated in a systematic manner until the required performance and flow characteristics are obtained.

3. RESULTS AND DISCUSSION

After the completion of the analyses, the post-process was conducted using ANSYS CFX-Post. The obtained compressor performance results are given in Figure 9.

Rotation Speed	10053.1000	[radian s^-1]
Mass Flow Rate	0.6780	[kg s^-1]
Inlet Volume Flow Rate	0.5844	[m^3 s^-1]
Input Power	123408.0000	[W]
Reference Radius	0.0493	[m]
Inlet Flow Coefficient	0.1211	
Exit Flow Coefficient	0.2780	
Head Coefficient	2.5869	
Work Input Coefficient	0.7402	
Total Pressure Ratio	4.6135	
Total Temperature Ratio	1.5933	
Total Isentropic Efficiency %	92.3842	
Total Polytropic Efficiency %	94.3214	

Figure 9. Compressor performance results

The relative Mach number contour at %50 span is given Figure 10. The comparison of the required parameters and the obtained parameters are given in Table 5.

Table 5. The required and the obtained parameters

Parameter	**Required Value**	**Obtained Value**
Mass Flow Rate, kg/s	$0.67 \leq \dot{m} \leq 0.69$	0.678
Total Pressure Ratio	$4.55 \leq PR \leq 4.65$	4.61
Total Isentropic Efficiency	$\eta \geq 0.87$	92.38
Surge Margin	≥ 15	29.106

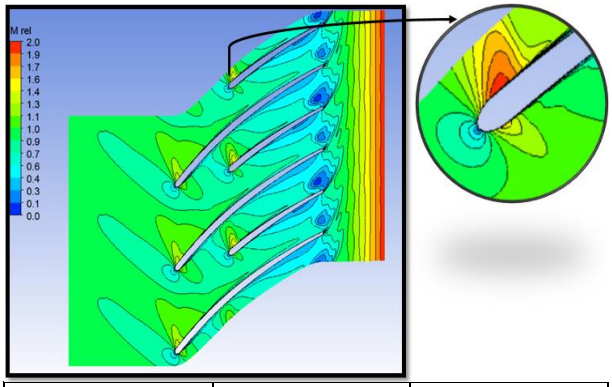

Figure 10. Relative Mach number at %50 span

The targeted mass flow rate, total pressure ratio and the rotational speed is quite high, which results in complicated flow characteristics and finally shock waves. This situation deteriorates performance and causes the rotor to operate in a narrower range [6]. It is known that blade thickness is affective on local acceleration [9], which also affects local Mach number. For this reason, especially in high-speed compressors, the leading edge is designed as thin as possible to minimize blade blockage and the effect of shock waves. The regions where the local Mach number is 1 or higher than 1, it is possible for a shock wave to develop at the leading edge [9]. As seen in Figure 10, sudden accelerations are obtained at blade leading edge. The reasons lying under this condition are the tip clearance and the high mass flow rate. These reasons result in the inlet relative Mach number to reach supersonic values which leads to shock waves [10]. As the flow goes from the leading edge towards the trailing edge, it can be seen that relative Mach number in the shroud region becomes near zero [11]. The vortex formed near the trailing edge causes the mass flow near the region to decrease and results in flow separation [12].

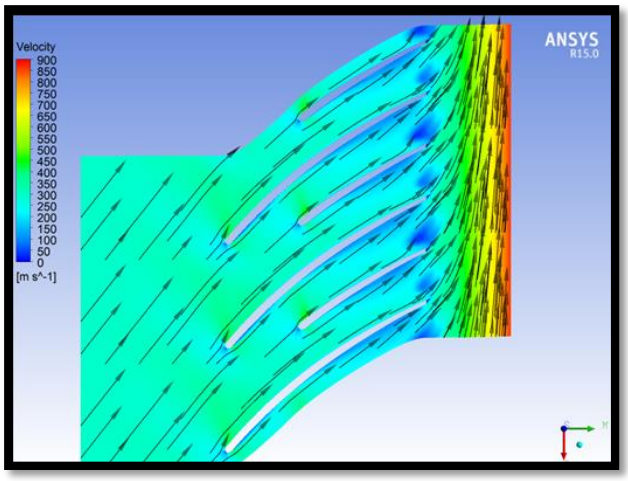

Figure 11. Velocity vectors and contour

From Figure 11, one can see that the flow progresses from the leading edge toward the trailing edge without any backflow or etc. The velocity increases from the leading edge through the trailing edge, which is an expected result.

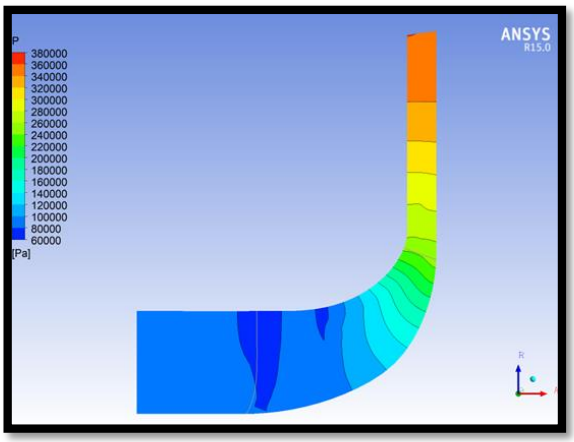

Figure 12. Pressure contour on meridional surface

The pressure is gradually increasing from the leading edge through the trailing edge. This is a consistent result as the operating principle of a compressor is taken into consideration.

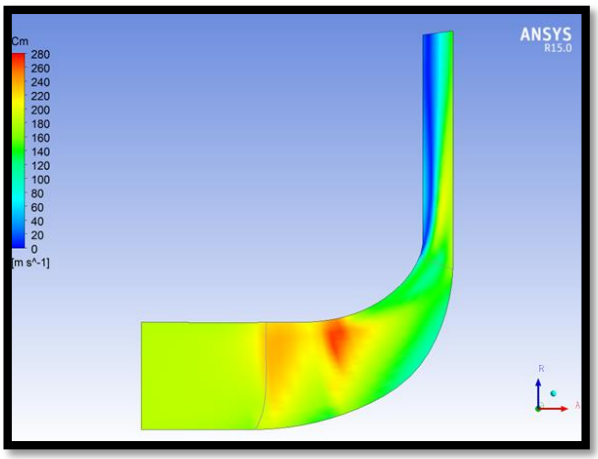

Figure 13. Meridional velocity contour on meridional surface

The meridional velocity contour on the meridional surface is given in Figure 13. The meridional velocity increases from the inlet to the outlet, which is consistent with the theoretical calculations performed. The sudden decrease obtained in the tip region is a result of tip clearance flow. This undesirable result, which leads to decrement in performance, can be prevented by the selection of a proper tip clearance value [13, 14, 15]. However, this value is fixed as a requirement in this study.

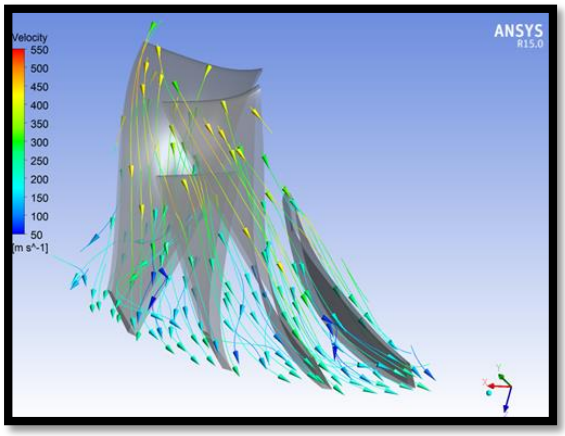

Figure 14. Velocity streamlines

The velocity streamlines are given in Figure 14 in a 3D view. It can be seen that the streamlines follow a proper path without any backflow.

4. EXPERIMENTAL RESULTS

The designed centrifugal compressor was manufactured and tested using a turbo jet engine which is currently being used commercially. For evaluation, the results of the compressor was compared with that of the commercial engine. Due to the confidentiality agreement, the details of the test stand and test procedure cannot be presented. Also, the obtained data is normalized and is not presented for the same reason.

The manufactured compressor can be seen in Figure 15.

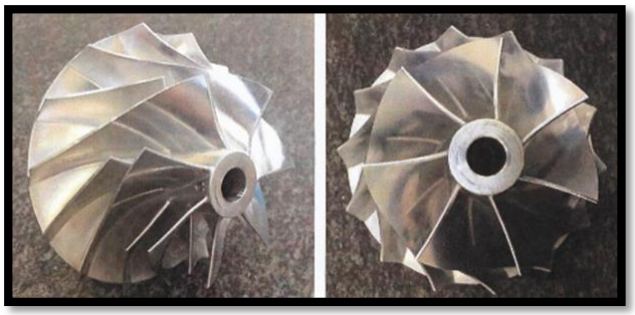

Figure 15. The manufactured compressor

4.1. Total Pressure Ratio

As it can be seen from Figure 16, the total pressure ratio of the designed impeller is very close to that of the test engine.

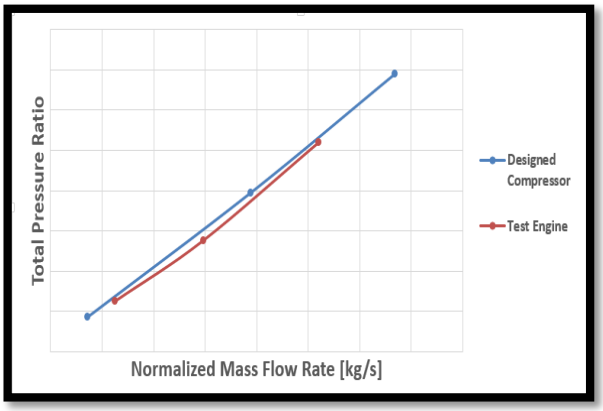

Figure 16. The normalized mass flow rate versus total pressure ratio

It can be seen from Figure 16 that the total pressure ratio increases with the increasing normalized mass flow rate. The normalization of the mass flow rate cannot be revealed due to confidentiality agreement. It is clear from the figure that the results of the designed compressor is quite matching with that of test engine.

The relationship between the normalized rotational speed and the mass flow rate is given in Figure 17.

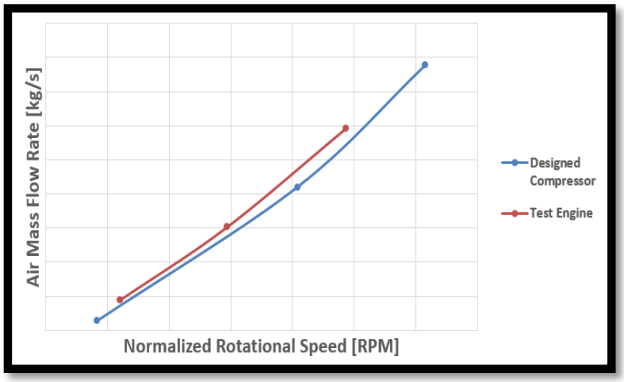

Figure 17. The normalized rotational speed versus mass flow rate

From Figure 17, one can see that with the increasing rotational speed, the mass flow rate of air increases correlatively. Again, it is obvious that the designed impeller gives similar results to that of the test engine.

The variation of the efficiency with respect to normalized rotational speed is given in Figure 18.

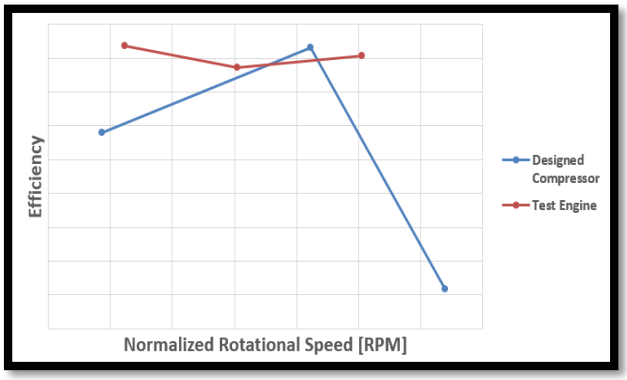

Figure 18. The normalized rotational speed versus efficiency

It can be seen from Figure 18 that the efficiency of the test engine varies in a narrower range with the increment in rotational speed compared to the designed impeller. However, speaking for the designed impeller, the efficiency decreases substantially in the maximum rotational speed. This situation can be stemmed from several reasons like calibration errors in the test procedure, etc.

5. CONCLUSION

Based on the conducted study, one can say that Computational Fluid Dynamics tools are a cheap and effective way to design a centrifugal compressor without the requirement of a test process. It was seen that the followed and described methodology for the design process gives accurate and consistent results; so, when starting a design process the authors recommend to performs the theoretical calculations initially to form a basis for the CFD analyses.

During the design process, it was obtained that even quite small variations in the blade geometry, especially blade angle distribution, blade number, etc. can cause substantial changes in the performance and flow parameters; so it is important for the designer to vary the design or geometrical parameters in such a way that the new design provides the required conditions. In conclusion, it was obtained that as the normalized mass flow rate increases total pressure ratio increases and the mass flow rate increases with the normalized rotational speed. Both the designed impeller and the test engine gives compatible results. Although the efficiency trends depending on normalized rotational speed differ from each other, the variation of efficiency values is in a small range. The difference can be arising from test/measurement/calibration errors or it can be stemmed from a main failure of the method of calculating efficiency.

REFERENCES

[1] Saravanamuttoo, H.I.H., Rogers, G.F.C., Cohen, H., Straznicky, P.V., "Gas Turbine Theory", (2001).

[2] Kulkarni, V.V., Anil, T.R., Rajan, N.K.S., "An Impeller Blade Analysis of Centrifugal Gas Compressor Using CFD", ***International Journal of Innovations in Engineering and Technology***, 7(4): (2016).

[3] Boyce, M.P., Principles of Operation and Performance Estimation of Centrifugal Compressors, (1993).

[4] https://www.quora.com/What-is-the-difference-between-a-centrifugal-compressor-and-a-screw-compressor

[5] Galerkin, Y., Reksrin, A., Drozdov, A., "2D and 3D Impellers of Centrifugal Compressors – Advantages, Shortcomings and Fields of Application", ***IOP Conference Series: Materials Science and Engineering***, 232(1): (2017).

[6] Tamaki, H., Unno, M., Kawakubo, T., Hirata, Y., "Aerodynamic Design of Centrifugal Compressor for AT14 Turbocharger", ***IHI Engineering Review***, 43(2): (2010).

[7] Damor, J.J., Patel, D.S., Thakkar, K.H., Brahmbhatt, P.K., "Experimental and CFD Analysis of Centrifugal Pump Impeller – A Case Study", ***International Journal of Engineering Research and Technology***, (2013).

[8] ANSYS CFX 15.0 User's Guide, ANSYS Inc., (2013).

[9] Japikse, D., "Centrifugal Compressor Design and Performance", Wilder VT, USA: Concepts ETI, (1996).

[10] Pakle, S., Jiang, K., "Design of a high-performance centrifugal compressor with new surge margin improvement technique for high speed turbomachinery", ***Propulsion and Power Research***, 7(1): (2018).

[11] He, X., Zheng, X., "Mechanisms of Sweep on the Performance of Transonic Centrifugal Compressor Impellers", ***Applied Sciences***, 7(10): 1081, 2017.

[12] Bogdanets, S., Blinov, V., Sedunin, V., Komarov, O., Skorohodov, A., "Validation of a CFD Model of a Single Stage Centrifugal Compressor by Local Flow Parameters", ***EPJ Web of Conferences; Les Ulis EDP Sciences***, 196: (2019).

[13] Zahed, A. H., Bayomi, N. N., "Design Procedure of Centrifugal Compressors", **ISESCO Journal of Science and Technology**, 10(17): (2014).

[14] Casey, M. V., Krahenbühl, D., Zwyssig, C., "The Design of Ultra-High-Speed Miniature Centrifugal Compressors", ***European Conference on Turbomachinery Fluid Dynamics and Thermodynamics ETC***, 10: (2013).

[15] Li, P. Y., Gu, C. W., Song, Y., "A New Optimization Method for Centrifugal Compressors Based on 1D Calculations and Analyses", ***Energies***, 8(5): 4317-4334, 2015.